Supplementary Table 1. Demographics of Included Patients

Total # Patients	57
Female	42
Male	15
Mean age +/- standard deviation	51.4 +/- 14.8 years
Mean Bern Score	3.53
Low Bern (0-2)	25
Intermediate Bern (3-4)	15
High Bern (5-8)	17

Supplementary Table 2. Location of Definitive CVFs Detected on Decubitus PC-CTM

Location (side or spinal level)	**Number of CVFs**
Left	13
Right	25
C8	1
T1	0
T2	1
T3	2
T4	1
T5	3
T6	4
T7	5
T8	2
T9	6
T10	7
T11	2
T12	3
L1	1

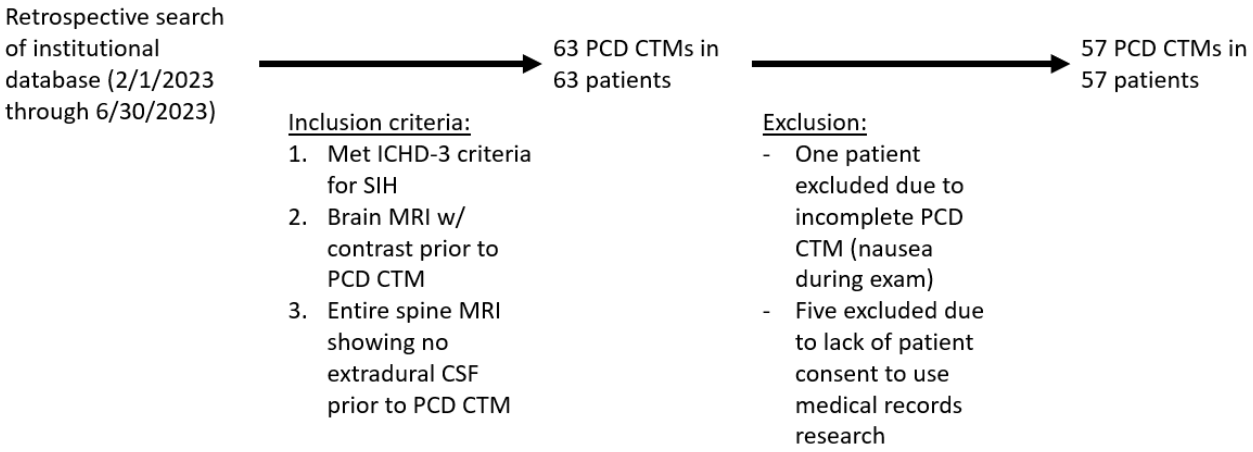

Supporting Flow Diagram. Illustration of the selection process for the patient cohort.

Supplementary Figure 4. Examples of definitive versus equivocal CVFs on PC-CTM in two patients (A-D versus E-H). The first patient had a previously negative decubitus DSM and decubitus dynamic CTM (A-B) showing a bilobed left T6 meningeal diverticulum but no evidence of CVF (A-B, arrows). Axial (C) and coronal (D) 0.2 mm T3D images from decubitus PC-CTM demonstrate a definite left T6 CSF-venous fistula involving the ventral IVVP (C-D, arrows). The second patient had a negative decubitus DSM (not shown). Axial and coronal 40 keV (E-F) and T3D (G-H) images from a PC-CTM demonstrate an equivocal left T5 CSF-venous fistula involving the left T5 IVVP (E-H, arrows). All images are windowed and leveled identically, highlighting the added value of 40 keV images for detecting subtle contrast opacification. In this case, the fistula was deemed equivocal rather than definitive, because the maximal attenuation of the draining vein on T3D images was between 100 HU and 199 HU.

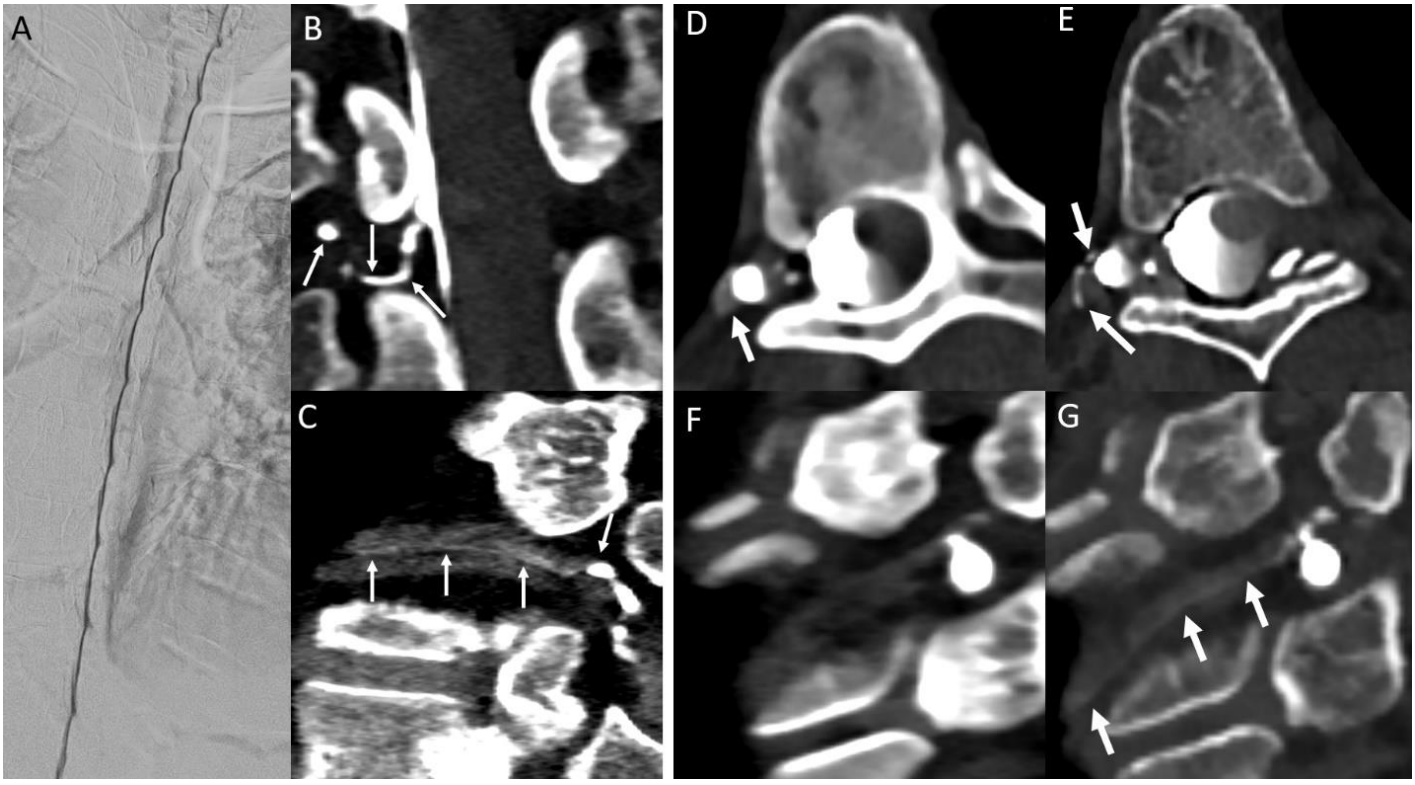

Supplementary Figure 5. Benefits of high spatial resolution in detecting and characterizing CVFs on PC-CTM in two separate patients (A-C versus D-G). The first patient (A-C) had a Bern score of 0 and initially underwent negative right lateral decubitus DSM (A). Coronal 40 keV image from his subsequent PC-CTM (B) shows a definitive right T9 CVF involving the IVVP and EVVP (B, arrows). Sagittal T3D reconstruction at 0.2 mm (C) shows an additional extremely thin column of contrast extending anteriorly in the paraspinal segmental vein (C, arrows), which was not apparent on 40 keV 0.4 mm images. In the second patient (D-G), axial and sagittal 0.4 mm 40 keV (D, F) and 0.2 mm T3D (E, G) show a right T6 CVF. Tiny veins around a meningeal diverticulum are well delineated at 0.2 mm (E, arrows) but appear amorphous on the 0.4 mm reconstructions (D, arrow). Moreover, the 0.2 mm sagittal T3D reconstruction shows a thin column of contrast in the right T6 paraspinal segmental vein (G, arrows), which is not clearly apparent on the 0.4 mm sagittal reconstructions (F).